Supramolecular Chemistry
Publication details, including instructions for authors and subscription information:
http://www.informaworld.com/smpp/title~content=t713649759

Kinetic and thermodynamic inclusion complexes of symmetric teramethyl-substituted cucurbit[6]uril with HCl salts of *N,N'*-bis(pyridylmethyl)-1,6-hexanediamine

Li He[a]; Jin-Ping Zeng[a]; Da-Hai Yu[a]; Hang Cong[a]; Yun-Qian Zhang[a]; Qian-Jiang Zhu[a]; Sai-Feng Xue[a]; Zhu Tao[a]
[a] Key Laboratory of Macrocyclic and Supramolecular Chemistry of Guizhou Province, Guizhou University, Guiyang, P.R. China

First published on: 31 August 2010

To cite this Article He, Li , Zeng, Jin-Ping , Yu, Da-Hai , Cong, Hang , Zhang, Yun-Qian , Zhu, Qian-Jiang , Xue, Sai-Feng and Tao, Zhu(2010) 'Kinetic and thermodynamic inclusion complexes of symmetric teramethyl-substituted cucurbit[6]uril with HCl salts of *N,N'*-bis(pyridylmethyl)-1,6-hexanediamine', Supramolecular Chemistry, 22: 10, 619 — 628, First published on: 31 August 2010 (iFirst)
To link to this Article: DOI: 10.1080/10610278.2010.510187
URL: http://dx.doi.org/10.1080/10610278.2010.510187

Supramolecular Chemistry
Vol. 22, No. 10, October 2010, 619–628

Taylor & Francis
Taylor & Francis Group

Kinetic and thermodynamic inclusion complexes of symmetric teramethyl-substituted cucurbit[6]uril with HCl salts of *N,N′*-bis(pyridylmethyl)-1,6-hexanediamine

Li He, Jin-Ping Zeng, Da-Hai Yu, Hang Cong, Yun-Qian Zhang, Qian-Jiang Zhu, Sai-Feng Xue and Zhu Tao*

Key Laboratory of Macrocyclic and Supramolecular Chemistry of Guizhou Province, Guizhou University, Guiyang 550025, P.R. China

(*Received 10 October 2009; final version received 15 July 2010*)

The host–guest interaction of symmetrical $\alpha,\alpha',\delta,\delta'$-tetramethyl-cucurbit[6]uril (TMeQ[6]) with the hydrochloride salts of *N,N′*-bis(4-pyridylmethyl)-1,6-hexanediamine (**P6**), *N,N′*-bis(3-pyridyl-methyl)-1,6-hexanediamine (**M6**) and *N,N′*-bis(2-pyridylmethyl)-1,6-hexanediamine (**O6**) was investigated via single crystal X-ray diffraction, ^{1}H NMR spectroscopy, electronic absorption spectroscopy and fluorescence spectroscopy. Single crystal X-ray diffraction showed that the hexyl moiety of **P6** or **M6** was incorporated in the cavity of TMeQ[6], while the two pyridylmethyl moieties of **O6** were incorporated in the TMeQ[6] cavity in the solid state. The ^{1}H NMR results in aqueous solution revealed that the TMeQ[6]-**P6** and TMeQ[6]-**M6** host–guest interaction systems produce a kinetic dumbbell-shaped inclusion complex at the initial stage and then an equilibrium pseudorotaxane-shaped inclusion complex as the only product after heating. However, only the pseudorotaxane-shaped inclusion complex was observed for the TMeQ[6]-**O6** host–guest interaction system. Aqueous absorption spectrophotometric analysis showed that the dumbbell-shaped inclusion complexes were stable at pH 5.6, had a host–guest ratio of 2:1 and formed quantitatively at $\sim 10^{11}$ l^2/mol^2 for the TMeQ[6]-**M6** and TMeQ[6]-**O6** systems. The transformation from dumbbell to pseudorotaxane-shaped inclusion complexes for the TMeQ[6]-**P6** and TMeQ[6]-**M6** host–guest systems yielded activation energies of 59.35 ± 1.55 and 78.7 ± 3.45 kJ/mol, respectively. The pseudorotaxane-shaped inclusion complexes were stable at pH 5.6, had a host–guest ratio of 1:1 and formed quantitatively at $\sim 10^7$ l/mol for the TMeQ[6]-**M6** and TMeQ[6]-**P6** systems.

Keywords: TMeQ[6]; *N,N′*-bis(pyridylmethyl)-1,6-hexanediamine; host–guest inclusion complexes; interaction models

Introduction

Rotaxanes and poly-rotaxanes have received considerable attention due to their unique topology, structures and interesting properties. They are the building blocks for important metal-organic solids having large pores or channels with controlled sizes and shapes and the ability to withstand exposure to various chemical environments (*1–5*). Their intriguing structures allow for potential applications in the fields of molecular devices, separation, catalysis and optoelectronics (*6–10*). A rotaxane is a super-molecule assembly consisting of three parts: rings, strings and stoppers. The ring is usually one of several organic hosts such as crown ethers (*11–13*), cyclophanes (*14*, *15*), calixarenes (*16*), cyclodextrins (*17–19*) or the cucurbit[*n*]uril family (*20–32*). Since the cucurbituril structure (Q[6]) was first reported in 1981, there have been numerous additions to the cucurbit[*n*]uril family (*20–32*). Cucurbit[*n*]urils are pumpkin-shaped macrocyclic compounds composed of *n* symmetrically arranged glycoluril units, covalently linked by 2*n* methylene bridges to form a rigid macro-cavitand with two highly polar carbonyl openings (*20*). The strong tendency to form host–guest complexes with aliphatic diammonium or polypyridyl ions by ion–dipole and hydrogen-bonding interactions makes Q[*n*] attractive building blocks for the construction of organic-metal frameworks (MOFs). Kim and co-workers demonstrated a series of 1D or 2D supramolecular assemblies and molecular necklaces through the formation of coordination complexes of metal ions with the pseudorotaxane of Q[6] and *N,N′*-bis(pyridylmethyl)-1,ω-alkylenediamine (*22, 33–38*). On the other hand, the guest with multiple functional groups could lead to kinetic vs. thermodynamic Q[*n*]-based self-sorting with high-fidelity recognition properties of natural systems (*39, 40*). This prompted us to study an approach to the non-covalent synthesis of a supramolecular assembly, based on a pseudorotaxane of a water-soluble alkyl-substituted cucurbit[6]uril with guest molecules containing multiple functional groups that have strong intermolecular interactions with the host.

In this work, we selected HCl salts of *N,N′*-bis(4-pyridylmethyl)-1,6-hexanediamine (**P6**), *N,N′*-bis(3-pyridyl-methyl)-1,6-hexanediamine (**M6**) and *N,N′*-bis(2-pyridylmethyl)-1,6-hexanediamine (**O6**) as guests that contain the two typical functional group's pyridyl rings and the 1,6-hexanediamine chain, which have a

*Corresponding author. Email: gzutao@263.net

ISSN 1061-0278 print/ISSN 1029-0478 online

DOI: 10.1080/10610278.2010.510187
http://www.informaworld.com

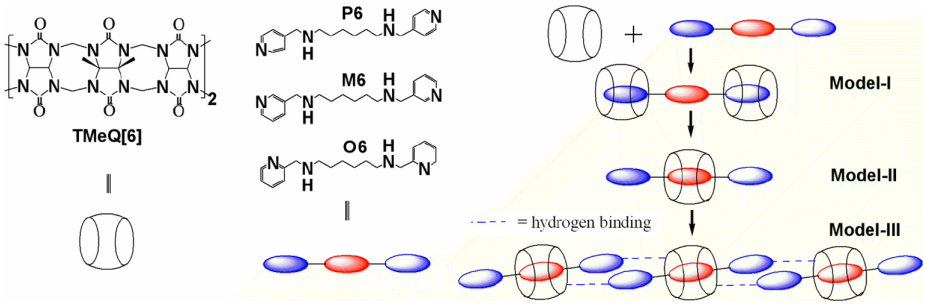

Scheme 1. Possible models of the related interaction systems.

suitable size for remaining in the cavity of the host TMeQ[6]. Our strategy involves the preparation of dumbbell or pseudorotaxane TMeQ[6] with the selected guests and then forming a polyrotaxane through intermolecular interactions such as ion–dipole, π–π stacking and hydrogen bonding (as shown in Scheme 1).

Experimental

General methods of synthesis guest and preparation of polyrotaxane

All commercially available chemicals are of reagent grade and used as received without further purification. ^{1}H NMR spectra were recorded on a Varian 400 spectrometer. Full visible absorption spectra and absorbance-time traces were obtained with a HP 8453A Diode-Array spectrophotometer thermostated to the desired temperatures, and UV-Visible ChemStation software was used to analyse the kinetic data. The data were routinely checked to ensure that the absorbance did not exceed 1.5 times the chosen wavelength range and that the data covered at least 2 *t*1/2 of reaction (usually more than 3–4 *t*1/2). All kinetic runs were performed in triplicate, using a concentration of the inclusion host–guest complex between 0.0002 and 0.0005 mol/l to achieve the desired absorbance change. TMeQ[6] was prepared and purified according to published procedures or those developed in our laboratory (*31*).

Preparation of HCl salts of N,N′*-bis(4-pyridylmethyl)-1,6-hexanediamine (P6),* N,N′*-bis(3-pyridyl-methyl)-1,6-hexanediamine (M6) and* N,N′*-bis(2-pyridylmethyl)-1,6-hexanediamine (O6)*

Guests **P6**, **M6** and **O6** were synthesised according to methods similar to those found in the literature (*41*). For example, hexamethylene diamine (1.16 g, 0.01 mol) and *p*-aldehydepyridine (2.15 g, 0.02 mol) were dissolved in 20 ml ethanol and refluxed for 5 h. To this solution, $NaBH_4$ (1.94 g, 0.05 mol) at ice bath was added slowly over 30 min and then stirred 8 h at room temperature. The solution was neutralised using HCl 37%, and precipitation was removed by filtration. The filtrate was further acidified using 37% HCl, and the organic impurities in the solution were extracted with chloroform twice. Excess NaOH was added to the aqueous solution, and the free **P6** was extracted using chloroform twice. After removing chloroform, the residue was dissolved in ethanol and acidified using 37% hydrochloric acid, and the precipitation (**P6**·2HCl) was collected by filtration. The yield of **P6**·2HCl was 65% (2.43 g); ^{1}H NMR (400 MHz, D_2O) *δ*: 8.725(d, 4H), 7.981(d, 4H), 4.428(s, 4H), 3.051(t, 4H), 1.619(s, 4H), 1.289(s, 4H). The yield of **M6**·2HCl was 58% (2.16 g); ^{1}H NMR (400 MHz, D_2O) *δ*: 8.437(s, 2H), 8.427(s, 2H), 7.808(d, 2H), 7.380(q, 2H), 4.101(s, 4H), 2.888(s, 4H), 1.527(s, 4H), 1.229(s, 4H). The yield of **O6**·2HCl was 89% (3.32 g);^{1}H NMR (400 MHZ, D_2O) *δ*: 8.589(d, 2H), 8.056(t, 2H), 7.619(d, 2H), 7.579(t, 2H), 4.364(s, 4H), 3.034(m, 4H), 1.580(s, 4H), 1.289(s, 4H).

Complexation of TMeQ[6] with the related guests salts in aqua solution

For the Q[6]s host–guest complexation study, 2.0 – 2.5×10^3 mmol samples of TMeQ[6] in 0.5 – 0.7 g D_2O with the [guest]/[Q[6]] ratio ranging between 1 and 100 were prepared. The ^{1}H spectra were recorded at 20°C on a VARIAN INOVA-400 spectrometer.

Preparation of single crystal of compound {TMeQ[6]-P6}$^{2+}$2Cl$^-$21H$_2$O (1)

A mixture of TMeQ[6] (0.41 g, 0.40 mmol) and **P6**·2HCl (0.0294 g, 0.80 mmol) in water (15 ml) was heated with stirring at 50° for 2 h. The solution was filtered and the filtrate was allowed to stand at room temperature for a month. Colourless X-ray quality crystals of the compound **1** were obtained from the solution with a yield of 30%. Anal. calcd for $C_{58}H_{114}N_{28}O_{33}Cl_2$: C, 38.65; H, 6.37; N, 21.76. Found: C, 38.92; H, 6.22; N, 22.08.

Preparation of single crystal of compound {TMeQ[6]-M6}$^{2+}$ 2Cl$^-$ 19(H$_2$O) (2)

To prepare crystals of compound **2**, water was used as the solvent due to the moderate water solubility of TMeQ[6].

A solution containing TMeQ[6] (0.41 g, 0.40 mmol) and **M6**·2HCl (0.0294 g, 0.80 mmol) in water (10 ml) was heated for 10 min, and then allowed to stand at room temperature. Rock X-ray quality crystals were formed after 3 weeks with a yield of 35%. Anal. calcd for $C_{58}H_{110}N_{28}O_{31}Cl_2$: C, 39.43; H, 6.28; N, 22.20. Found: C, 38.27; H, 6.47; N, 21.49.

Preparation of single crystal of compound {2TMeQ[6]-O6}$^{2+}$ 2Cl$^-$ 36(H_2O) (3)

A solution containing TMeQ[6] (0.41 g, 0.40 mmol) and **O6**·2HCl (0.0294 g, 0.80 mmol) in water (10 ml) was heated for 10 min and then allowed to stand at room temperature. Rock X-ray quality crystals were formed after 3 weeks with a yield of 25%. Anal. calcd for $C_{98}H_{188}N_{52}O_{60}Cl_2$: C, 37.66; H, 6.06; N, 23.30. Found: C, 37.93; H, 5.83; N, 23.87.

X-ray crystal structure determination of compounds 1–3

A suitable corresponding single crystal ($\sim 0.2 \times 0.2 \times 0.1$ mm^3) was picked up with paratone oil and mounted on a Burker Apex2 CCD diffractometer equipped with a graphite-monochromated Mo Kα ($\lambda = 0.71073$ Å) radiation source and a nitrogen cold stream (-50°C). The data were corrected for Lorentz and polarisation effects (SAINT) (*42*), and semi-empirical absorption corrections based on equivalent reflections were applied (SADABS) (*42*). The structure was elucidated by direct methods and refined by the full-matrix least-squares method on F^2 (SHELXTL) (*43*). All the non-hydrogen atoms were refined anisotropically, and hydrogen atoms were added to their geometrically ideal positions. Partial water molecules in the compounds are disordered and normalised, and for compounds **1** and **3**, the OW atoms have been given an occupancy factor of 0.5, and for compound **2**, the OW atoms have been given an occupancy factor of 0.3 or 0.7. Particularly, in compound **2**, the carbon atoms containing C51, C51′ and C60, C61 in the hexanediamine moiety of the guest **M6** are disordered and all have been given an occupancy factor of 0.5. Details of the crystal parameters, data collection and refinements for complexes **1**–**3** are summarised in Table 1. Additionally, the crystallographic data for the reported structures were recorded in the Cambridge Crystallographic Data Centre as supplementary publication no. CCDC 679223 (**1**), 679226 (**2**) and 749212 (**3**). These data can be obtained free of charge via http://www.ccdc.cam.ac.uk/data_request/cif, or by emailing data_request@ccd c.cam.ac.uk, or by contacting the Cambridge Crystallographic Data Centre, 12, Union Road, Cambridge CB2 1EZ, UK; Fax: 44 1223 336033.

Results and discussion

Synthesis

We first demonstrated the controlled synthesis of the symmetrical TMeQ[6] (*31*) utilising the readily available dimer of glycoluril. Condensing the diether of dimethyl glycoluril with the glycoluril dimer produces TMeQ[6], and the **P6**, **M6** and **O6** guests were synthesised according to the literature (*41*).

Table 1. Crystallographic data for the compounds **1**–**3**.

Compounds	**1**	**2**	**3**
Empirical formula	$C_{58}H_{114}Cl_2N_{28}O_{33}$	$C_{58}H_{110}Cl_2N_{28}O_{31}$	$C_{98}H_{188}Cl_2N_{52}O_{60}$
Formula weight	1802.67	1776.64	3125.90
Crystal system	Monoclinic	Triclinic	Triclinic
Space group	*P* 2$_1$/*c*	*P*-1	*P*-1
a (Å)	14.686(3)	12.199(2)	11.8480(17)
b (Å)	20.098(5)	12.238(2)	12.9541(19)
c (Å)	14.503(3)	26.488(5)	23.084(3)
α (°)	90.00	88.939(2)	103.445(4)
β (°)	111.058(3)	85.608(2)	91.127(5)
γ (°)	90.00	84.498(2)	93.743(5)
V (Å^3)	3995.0(16)	3924.4(13)	3436.3(9)
Z	2	2	1
λ (Å)	0.71073	0.71073	0.71073
D calcd, g cm^{-3}	1.499	1.495	1.511
T (K)	223	223	223
μ (Mo Kα), mm^{-1}	0.186	0.186	0.162
Unique reflections	6961	13369	12026
Observed reflections	3899	10699	5902
Parameters	586	1126	1010
R_{int}	0.0507	0.0212	0.0950
$R[I > 2\ \delta\ (I)]$[a]	0.1102	0.0836	0.0842
$wR[I > 2\ \delta\ (I)]$[b]	0.3261	0.2672	0.2239

[a] Conventional *R* on F*hkl*: $\Sigma||Fo|-|Fc||/\Sigma|Fo|$.
[b] Weighted *R* on $|Fhkl|^2$: $\{\Sigma[w(Fo^2 - Fc^2)^2]/\Sigma[w(Fo^2)^2]\}^{1/2}$.

Crystallographic description of the structures and interaction models of TMeQ[6] with the selected guests

As mentioned above, the selected guests have multiple functional groups, like the pyridyl ring and hexylene chain, which result in intermolecular interactions with the host TMeQ[6] (*31*, *41*, *44*, *45*). Thus, TMeQ[6] interactions could include the pyridyl moiety or hexyl chain of the guest to form either a pseudorotaxane or a dumbbell-shaped inclusion complex (as shown in Scheme 1 model I or model II). Furthermore, the pseudorotaxane inclusion complexes may form a supramolecular assembly through π–π stacking and hydrogen bonding in the solid state (as shown in Scheme 1 model III). In this work, we investigated the interaction between the host and guests, both in the solid state and in solution. Generally, crystals of a host–guest inclusion complex define the thermodynamic structure of the complex. Although the three guests have similar structures, the crystal structures of the host–guest inclusion complexes of TMeQ[6] suggest different interaction models. The TMeQ[6]-**P6** or **M6** interaction systems have pseudorotaxane host–guest inclusion complexes, while the TMeQ[6]-**O6** interaction system has a dumbbell host–guest inclusion complex. Figure 1 shows the crystal structures of (a) TMeQ[6]-**P6**, (b,c) TMeQ[6]-**M6** and (d) TMeQ[6]-**O6** inclusion complexes corresponding to the compounds **1**–**3**, respectively.

When the host TMeQ[6] includes the hexylene chain of the protonated **P6** or **M6** guests, a pseudorotaxane-like inclusion complex is formed, while for the pyridyl moiety of the **O6**, a dumbbell-like inclusion complex is the result. Despite the difference in the interaction structure of the three host–guest inclusion complexes, the protonated amino groups of the guests interact with the portal carbonyl oxygen atoms through the ion–dipole interaction and the hydrogen bonding. For the TMeQ[6]-**P6** inclusion complex, the protonated nitrogen atom N29 interacted with the portal carbonyl oxygen atoms O1, O2 and O3 (N29···O1, 2.900(6)Å; N29···O2, 2.819(6)Å; N29···O3, 2.888(6)Å). For the TMeQ[6]-**M6** inclusion complex, similar interactions are observed, the protonated nitrogen atoms N26 and N28 interacted with the portal carbonyl oxygen atoms O3 and O4 (N26···O3, 2.771(4)Å; N26···O4, 2.960(4)Å) and O10 and O11 (N28···O10, 2.990(4)Å; N28···O11, 2.807(4)Å). For the TMeQ[6]-**O6** inclusion complex, the protonated nitrogen atom N26 interacted with the portal carbonyl oxygen atoms O1, O2 and O6 (N26···O1, 2.958(7)Å; N26···O2, 2.883(6)Å; N26···O6, 3.063(7)Å). However, the two amino nitrogen atoms N29 or N58 of the guest interact with both portals of the TMeQ[6]-**P6** and TMeQ[6]-**M6** host systems, while the two amino nitrogen atoms N26 interact with one of the

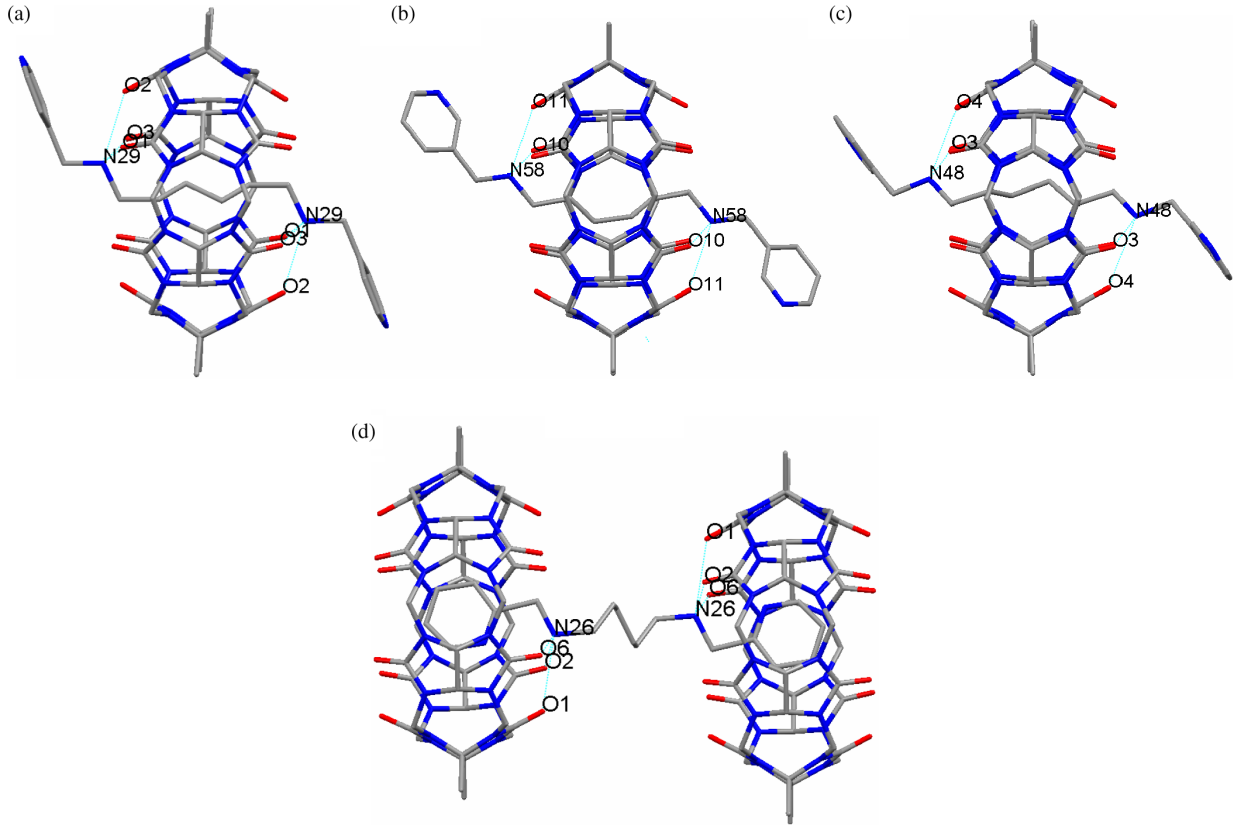

Figure 1. X-ray structure of host–guest inclusion complexes of (a) TMeQ[6]-**P6**, (b) and (c) TMeQ[6]-**M6** and (d) TMeQ[6]-**O6**.

portal carbonyl oxygen atoms of the two TMeQ[6]s hosts (refer to Figure 1(a)–(d)).

In Scheme 1, the pseudorotaxane complexes form a 1D supramolecular chain via π–π stacking of the protruded pyridyl moieties between the neighbouring pseudorotaxane complexes (model III). Indeed, such a supramolecular assembly can be observed in compound **1**, and the distance of the adjacent pyridyl planes is 3.554(4)Å (face to face) as shown in Figure 2(a). In addition, two pairs of latticed water molecules O10 and O15W interact with the pyridyl nitrogen N23 and carbonyl oxygen O5 through hydrogen bonding, which further strengthens the interaction between the neighbouring pseudorotaxane complexes and forms a 1D supramolecular assembly. As described above, there are two different pseudorotaxane complexes in compound **2**. Although, there are two different 1D supramolecular assemblies in compound **2**, the π–π stacking between the neighbouring pseudorotaxane complexes is not observed. Figure 2(b) and (c) show the two different 1D supramolecular assemblies b and c. In assembly b, the neighbouring host–guest complexes are connected by two latticed water molecules O5W through hydrogen bonding, and the distance between the two neighbouring complexes is 12.199 Å. In assembly c, the neighbouring host–guest complexes are also connected by two latticed water molecules O6W via hydrogen bonding, and the distance between the two neighbouring complexes is 12.238 Å. However, for compound **3**, the neighbouring dumbbell inclusion complexes are connected by water molecules that form a complicated hydrogen-binding network among themselves as well as the water molecules coordinated to the portal carbonyl oxygen atoms.

^{1}H NMR spectroscopic description of interaction models and transformation of the inclusion complexes of TMeQ[6] with the selected guests

As shown in Scheme 1, the guests used in this work have multiple functional groups that were shown to be suitable for the Q[6]s inclusion (*41*, *45*). When the host TMeQ[6] interacts with any of the selected guests, it must first incorporate the pyridyl moiety of the guest and then move on to the hexylene chain. However, the host TMeQ[6] exhibits a significant difference in selectivity for these functional groups, and the hexylene chain results in a more stable complex for the TMeQ[6]-**P6** or **M6** systems than the pyridyl moiety, while the pyridyl moiety is more stable for the TMeQ[6]-**O6** system (*46–49*).

The ^{1}H NMR results from the TMeQ[6]-**M6** system are now given in detail. Figure 3 shows the ^{1}H NMR spectra for the host TMeQ[6] in D_2O (a), the protonated **M6** in D_2O recorded in the presence of 4.0 (b), 2.2 equiv. of the host TMeQ[6] (c), and in the absence of the host TMeQ[6] (f). Figure 3(d) and (e) shows the samples corresponding to Figure 3(c) heated at 70°C for 10 min and 2 h, respectively. When TMeQ[6] and **M6** are combined in a ratio of 4:1, only one set of proton resonances of **M6** is observed in the ^{1}H NMR spectrum (Figure 3(b)). The cavity-bound pyridyl moiety proton

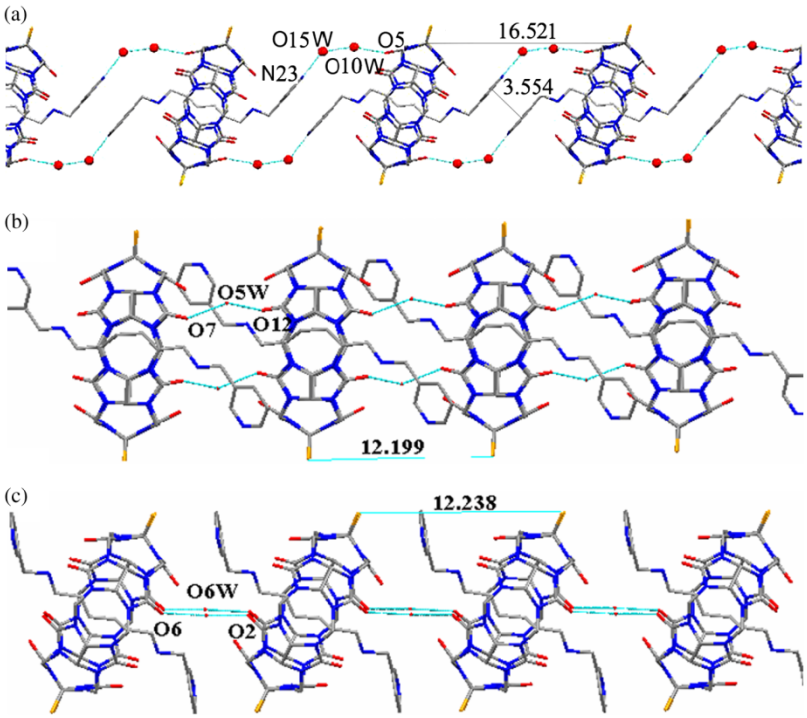

Figure 2. The supramolecular assemblies based on the pseudorotaxane complexes in the compound (a) **1** and (b) and (c) **2**.

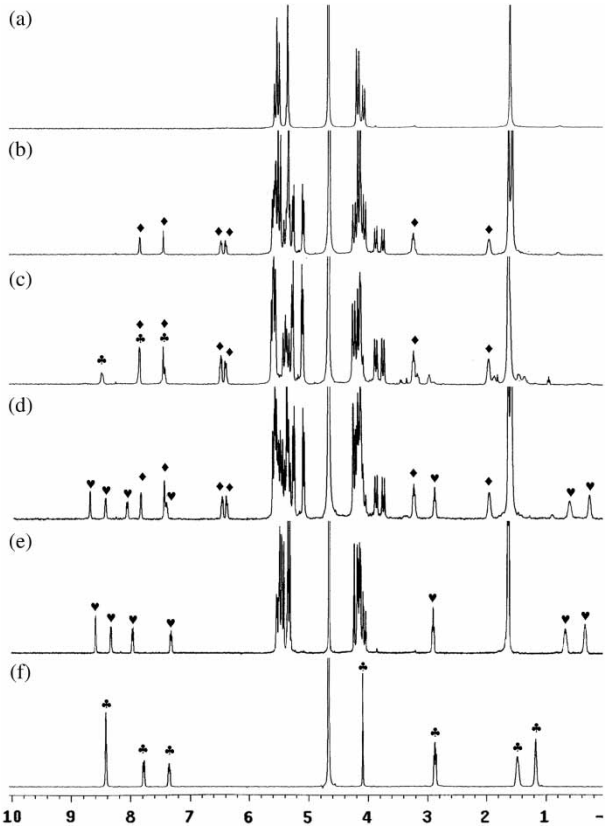

Figure 3. ^{1}H NMR spectra of (a) the host TMeQ[6] in D_2O, the protonated **M6** in D_2O recorded in the presence of (b) 4.0, (c) 2.2 equiv. of the host TMeQ[6] and (f) in the absence of the host TMeQ[6], (d) and (e) corresponding to the sample of (c) after heating at 70°C for 10 min and 2 h, respectively.

resonances (indicated by diamonds) occur upfield of the unbound pyridyl (indicated by club in Figure 1(f)) by 0.6–1.4 ppm, while a downfield shift between 0.3 and 0.4 ppm for the hexylene protons (indicated by diamonds) is also observed. This indicates that the hexylene protons are at the portals in the deshielding zone of the carbonyls. When the proportion of **M6** is increased to about 0.5, two sets of proton resonances for **M6** can be seen in the ^{1}H NMR spectrum (Figure 3(c)), one set (indicated by diamonds) is identical to that shown in Figure 3(b), and another set (indicated by club) is similar to that of the unbound guest as shown in Figure 3(f). A comparison of the integrals of the protons of the bound **M6** with the protons of TMeQ[6] reveals that the inclusion complex has a host–guest ratio of 2:1. Thus, a dumbbell-shaped host–guest inclusion complex can be formed under these conditions. It is interesting that when the sample shown in Figure 3(c) was heated at 70°C for 10 min, it gave an ^{1}H NMR spectrum as shown in Figure 3(d), which produced two sets of resonances for the protons of **M6**. One set (indicated by diamonds) is identical to that observed in Figure 3(b), and another set is new (indicated by hearts), with upfield shifts of about 0.9 ppm for the centre hexylene protons and downfield shifts of about 0.2 ppm for pyridyl protons of **M6,** suggesting that a pseudorotaxane-shaped inclusion complex is formed. Figure 3(e) shows the ^{1}H NMR spectrum of the same sample after heating for two more hours at 70°C, which shows only one set of proton resonances for the **M6** guest and corresponds to the new set as shown in Figure 3(e). This indicates that the dumbbell-shaped host–guest inclusion complex is converted irreversibly into the pseudorotaxane-shaped host–guest inclusion complex, and the former is a kinetic product while the latter is a thermodynamic product. Similar results are observed for the TMeQ[6]-**P6** system (see SI-Figure 1 in the Supporting Information, available online).

Figure 4 shows the ^{1}H NMR spectra of (a) the host TMeQ[6] in D_2O, protonated **O6** in D_2O recorded in the presence of (b) 5.4, (c) 1.9, (d) 0.9 equiv. of the host TMeQ[6] and (f) in the absence of the host TMeQ[6]. Figure 4(e) shows the ^{1}H NMR spectrum corresponding to the single crystals of compound **3,** which was heated at 90°C for 35 min. Compared to the unbound guest, only one set of the bound **M6** is observed in all the ^{1}H NMR spectra, even in the heated samples. The cavity-bound pyridyl moiety proton resonances (upfield shift by 0.8–1.4 ppm) and the portal-bound hexylene proton resonances (downfield shift between 0.2 and 0.4 ppm) indicate that a dumbbell-shaped host–guest inclusion complex is formed. The comparison of the integrals of a 2:1 host–guest ratio further confirms this interaction model for the TMeQ[6]-**O6** system.

Generally, there are two steps in the formation of the inclusion complexes of TMeQ[6] with the selected guests.

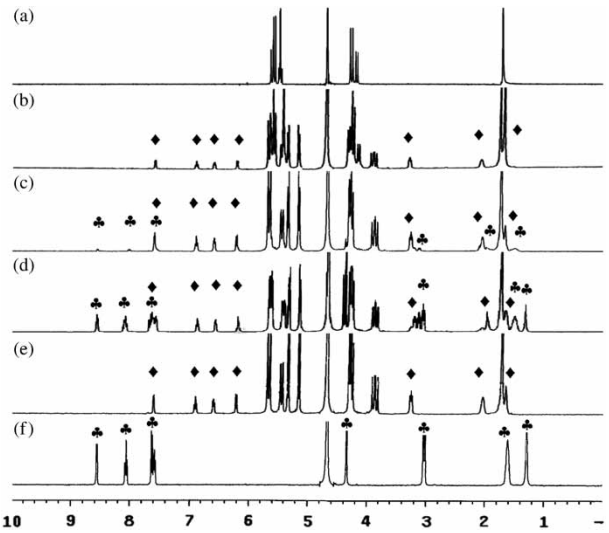

Figure 4. ^{1}H NMR spectra of (a) the host TMeQ[6] in D_2O, the protonated **O6** in D_2O recorded in the presence of (b) 5.4, (c) 1.9, (d) 0.9 equiv. of the host TMeQ[6], (f) in the absence of the host TMeQ[6] and (e) corresponding to the single crystals of the compound **3**, which was heated at 90°C for 35 min.

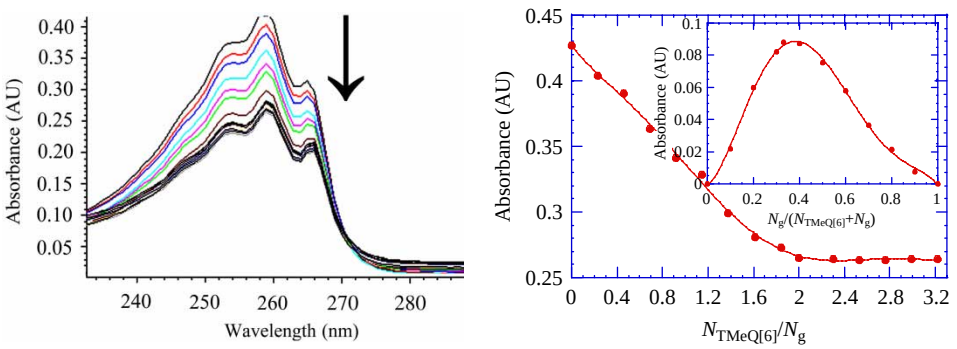

Figure 5. Electronic absorption spectra of **O6**·2HCl in the presence of increasing concentrations of TMeQ[6] (left) and corresponding absorbance vs. $N_{TMeQ[6]}/N_{\mathbf{O6}\cdot 2HCl}$ curve and ΔA vs. $[N_{TMeQ[6]}/(N_{TMeQ[6]} + N_{\mathbf{O6}\cdot 2HCl})]$ (inset) at $\lambda_{max} = 258$ nm (right).

First, the two hosts TMeQ[6] include the pyridyl moieties and form kinetic dumbbell inclusion complexes, and then one TMeQ[6] moves on the hexylene chain to form a thermodynamic pseudorotaxane inclusion complex. The formation of the inclusion complexes for the TMeQ[6]-**P6** and TMeQ[6]-**M6** systems is consistent with this process. However, the formation of the inclusion complexes for the TMeQ[6]-**O6** system seems to stop at the first step, and only the dumbbell inclusion complex is observed. The position of pyridyl nitrogen in the guests is the reason for such a difference in the formation of inclusion complexes in different host–guest systems. We will discuss this unique phenomenon below.

Spectrophotometric analysis on the interaction and kinetics of the transformation of the dumbbell to the pseudorotaxane of TMeQ[6]-guest

To quantify the interaction details of the TMeQ[6] host and the guests, aqueous absorption spectrophotometric analysis was used to estimate the stability of the inclusion complexes and the transformation from dumbbell to pseudorotaxane. Figure 5(a) shows the variation in the UV spectra of aqueous solutions containing a fixed concentration of **O6** and variable concentrations of TMeQ[6] at pH = 5.6 and at room temperature. The absorption spectra of the guest (TMeQ[6] shows no absorbance within the range of >210 nm) exhibit progressively lower absorbances as the ratio of $N_{TMeQ[6]}/N_{\mathbf{O6}\cdot 2HCl}$ is increased.

The absorbance (A) vs. the ratio of moles of TMeQ[6] and **O6** ($N_{Me4Q[6]}/N_{\mathbf{O6}\cdot 2HCl}$) data can be fitted to a 2:1 binding model for the TMeQ[6]-**O6**·2HCl system at λ_{max} 259 nm (Figure 5(b)). The inset shows the absorbance change (ΔA) vs. ratio of $[N_{TMeQ[6]}/(N_{TMeQ[6]} + N_{\mathbf{O6}\cdot 2HCl})]$ data, which can also be fitted to a 2:1 binding model. This behaviour is consistent with the results from both the ^{1}H NMR and single crystal structure studies. The data are used to calculate the binding constant (K) of 3.43×10^{11} l^2/mol^2 for the TMeQ[6]-**O6** inclusion complex. Similar experiments were performed for the TMeQ[6]-**M6** and TMeQ[6]-**P6** systems. The absorption spectra of the guest exhibited progressively lower absorbances as the ratio of $N_{TMeQ[6]}/N_{\mathbf{M6}\cdot 2HCl}$ is increased. Both of the absorbance (A) vs. the ratio of moles of the host TMeQ[6] to the guest **M6** ($N_{Me4Q[6]}/N_{\mathbf{M6}\cdot 2HCl}$) data and the absorbance change (ΔA) vs. the ratio of $[N_{TMeQ[6]}/(N_{TMeQ[6]} + N_{\mathbf{M6}})]$ data can be fitted to a 2:1 binding model under the same conditions (pH 5.6 and room temperature). The binding constant (K) of the TMeQ[6]-**M6** inclusion complex was 1.67×10^{11} l^2/mol^2 (see SI-Figure 2 in the Supporting Information, available online). Although the absorption spectra of the guest showed some changes indicating the conversion of the dumbbell inclusion complex into the pseudorotaxane inclusion complex, the differences of the absorbance as the ratio of $N_{TMeQ[6]}/N_{\mathbf{P6}\cdot 2HCl}$ were too small to calculate the binding constant for the TMeQ[6]-**P6** inclusion complex (referring to SI-Figure 3 in Supporting Information, available online).

According to ^{1}H NMR analysis for the TMeQ[6]-**P6** and TMeQ[6]-**M6** systems, the dumbbell inclusion complex can be irreversibly converted to the pseudorotaxane inclusion complex. These conversions can be also demonstrated via the absorption spectra changes of the guest. The corresponding observed rate constants at different temperatures and the observed activation energies for these host–guest interaction systems are summarised in Table 2. Figure 6(a) and (b) shows the absorption bands of TMeQ[6]-

Table 2. Summary of kinetics of the corresponding host–guest interaction systems.

1 TMeQ[6]-**M6** k_{obsd} ($M^{-1}s^{-1}$)/temp.	2 TMeQ[6]-**P6** k_{obsd} ($M^{-1}s^{-1}$)/temp.
1.12×10^{-5}/298 K	6.67×10^{-5}/298 K
3.58×10^{-4}/333 K	8.93×10^{-4}/333 K
5.30×10^{-4}/338 K	1.31×10^{-3}/338 K
8.28×10^{-4}/342 K	1.79×10^{-3}/342 K
1.26×10^{-3}/347 K	2.39×10^{-3}/347 K
2.00×10^{-3}/355 K	3.32×10^{-3}/355 K
E_{obsd}	E_{obsd}
78.7 ± 3.45 kJ/mol	59.35 ± 1.55 kJ/mol

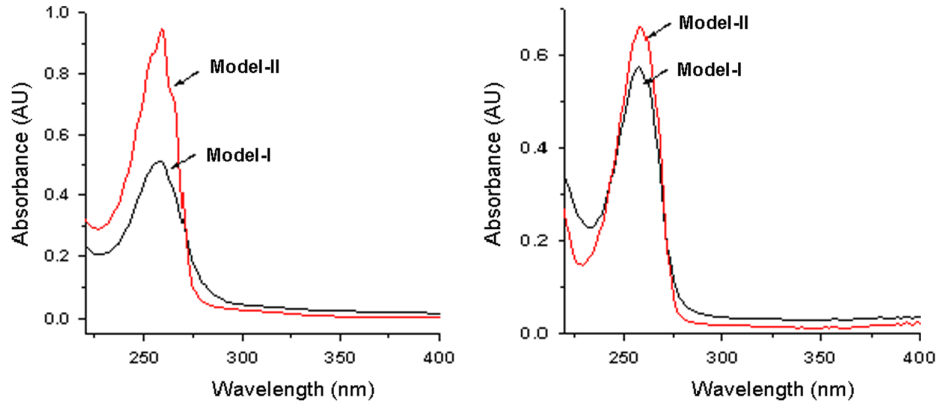

Figure 6. The absorption bands of TMeQ[6]-**M6** (left) and TMeQ[6]-**P6** (right) with a 2:1 host:guest ratio at initial and final stages at 333 K.

M6 and TMeQ[6]-**P6** at a 2:1 host–guest ratio in the initial and final stages at 333 K. Obviously, the absorption spectra of the guests exhibited increased absorbance with time and yielded the observed rate constants (k_{obsd}) which is 3.58×10^{-4} and $8.93 \times 10^{-4}\,M^{-1}\,s^{-1}$ at 333 K, respectively. The observed rate constant (k_{obsd}) increases with temperature (referring to Table 2). The activation energy for the dumbbell inclusion complex to the pseudorotaxane inclusion complex is easily determined from the kinetic data, and there is about 20 kJ/mol difference between the TMeQ[6]-**M6** and TMeQ[6]-**P6** systems (referring to Table 2, columns 1 and 2). The calculated rate constants at room temperature (298 K) are 1.12×10^{-5} and $6.67 \times 10^{-5}\,M^{-1}\,s^{-1}$ respectively, which is about 100 times slower than those at 355 K (referring to Table 2, columns 1 and 2).

Figure 7 shows the variation in the UV spectra of aqueous solutions containing a fixed concentration of the guest **P6** or **M6** and variable concentrations of the host TMeQ[6] at pH = 5.6, after heating half an hour at 90°. The absorption spectra of the guest exhibit progressively upper absorbances as the ratio of $N_{TMeQ[6]}/N_{\mathbf{P6}\cdot 2HCl}$ or $N_{\mathbf{M6}\cdot 2HCl}$ is increased (Figure 7(a) and (c)). The absorbance (A) vs.

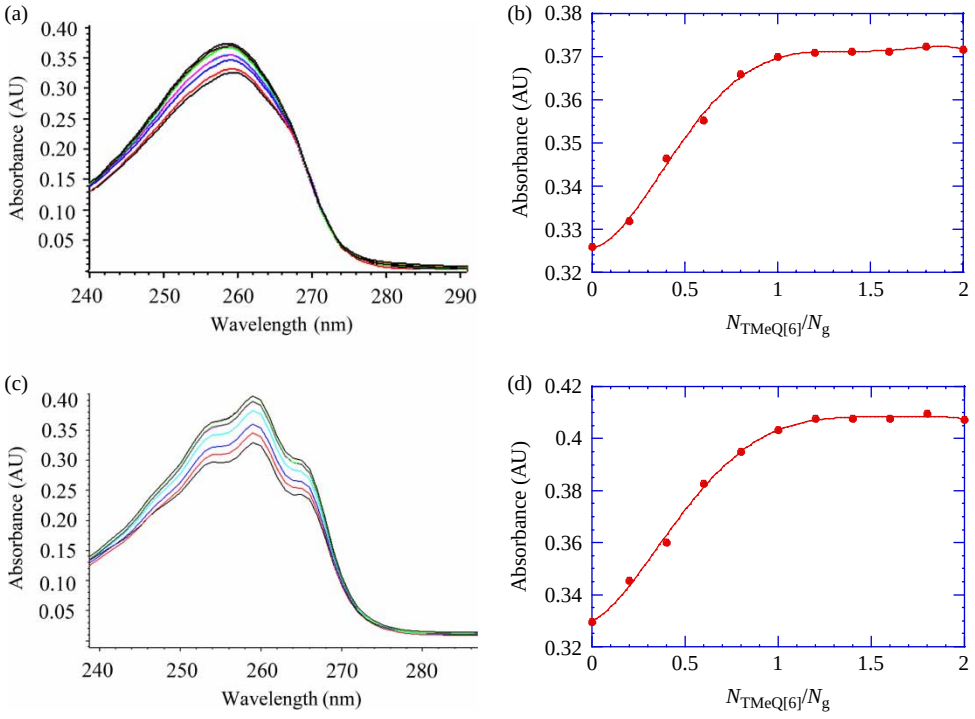

Figure 7. (a) Electronic absorption spectra of **P6**·2HCl in the presence of increasing concentrations of TMeQ[6], (b) corresponding absorbance vs. $N_{TMeQ[6]}/N_{\mathbf{P6}\cdot 2HCl}$ curve at $\lambda_{max} = 259$ nm, (c) electronic absorption spectra of **M6**·2HCl in the presence of increasing concentrations of TMeQ[6] and (d) corresponding absorbance vs. $N_{TMeQ[6]}/N_{\mathbf{M6}\cdot 2HCl}$ curve at $\lambda_{max} = 259$ nm.

ratio of moles of TMeQ[6] and **P6** or **M6** ($N_{Me4Q[6]}/N_{\mathbf{P6}\cdot \text{or } \mathbf{M6}\cdot 2HCl}$) data can be fitted to a 1:1 binding model for both of the TMeQ[6]-**P6** or **M6**·2HCl systems at λ_{max} 259 nm (Figure 7(b) and (d)), and these behaviours are consistent with the results from both of the ^{1}H NMR and single crystal structure studies. The measured data yield calculated binding constants (K) of 4.91×10^7 l/mol for the TMeQ[6]-**P6** inclusion complex and 4.89×10^7 l/mol for the TMeQ[6]-**M6** inclusion complex.

We investigated the interaction of TMeQ[6] with the HCl salts of **P6**, **M6** and **O6**, and the experimental results showed that the interaction behaviour of TMeQ[6]-**P6** and TMeQ[6]-**M6** was quite different from the TMeQ[6]-**O6** system, although the structures of the three guests were nearly identical. When TMeQ[6] includes the pyridyl moieties of **P6** or **M6**, a kinetic dumbbell-shaped inclusion complex is initially formed, which is converted irreversibly to an equilibrium pseudorotaxane-shaped inclusion complex after heating or sitting for a long time, while the kinetic and thermodynamic host–guest inclusion complexes are always dumbbell shaped for the TMeQ[6]-**O6** host–guest system. To show that the difference of the position of nitrogen of pyridyl moieties of the guests causes the different interaction properties for the three host–guest systems, we used the B3LYP/STO-3G method in Gaussian 03 to estimate the process of the guest ingression and egression of the cavity of TMeQ[6] (see SI-Figures 4 and 5 in the Supporting Information, available online). The profiles of the relative potential energy vs. the distance between the geometric centre of the guest and the dummy atom (d,Å) showed two peaks corresponding to the stages that the pyridyl moiety moves at the portal area of TMeQ[6] and leads to the geometric strain of the host–guest system, with no clear difference in the selectivity of the TMeQ[6] between the pyridyl moiety or hexylene chain. However, our previous work showed that the ···N—C—C—N^+···guest structure, such as HCl salts of 2-(aminomethyl)pyridine, 2,2′-dipyridine, always led to the formation of a stable inclusion complex with Q[6], while the ···N—C—C—C—N^+···guest structure, such as the HCl salt of 2-(aminoethyl)pyridine, cannot form an inclusion complex (*45*). This could be due to the 'clamp effect' of the two nitrogen atoms that interact with the portal carbonyl oxygen atoms, which forms a stable inclusion host–guest complex, and leads to the formation of a stable inclusion host–guest complex.

Conclusion

In this work, we demonstrated three host–guest interaction systems, TMeQ[6]-**P6**, TMeQ[6]-**M6** and TMeQ[6]-**O6**. The three guests used in this work offer multiple functional groups that can develop intermolecular interactions with TMeQ[6]. However, the difference of the position of nitrogen of pyridyl moieties of the guests leads to the different interaction properties for the three TMeQ[6]-**P6**, TMeQ[6]-**M6** and TMeQ[6]-**O6** systems. The 'clamp effect' of the **O6** guest blocks the TMeQ[6] host move on the hexylene chain and leads to form a pseudorotaxane-shaped inclusion complex only. Therefore, the guests, which have ···N—C—C—N^+···structure characteristic, like **O6**, cannot be used to further synthesise the so-called 'molecular necklace' or MOFs. While the **P6**, **M6** guests interact with TMeQ[6] and form a pseudorotaxane thermodynamic inclusion complex, the two pyridyl moieties protruding from the two opening portals, could further coordinate with different metal ions and form novel 'molecular necklace' or MOFs, which is our next aim.

Acknowledgements

We acknowledge the support of the National Natural Science Foundation of China (No. 20662003 and 20961002), the International Collaborative Project of Guizhou Province (No 2007400108) and the Foundation of the Governor of Guizhou Province.

References

(1) Abrahams, B.F.; Hoskins, B.F.; Michail, D.M.; Robson, R. *Nature* **1994**, *369*, 727–729.
(2) Yaghi, O.M.; Li, G.; Li, H. *Nature* **1995**, *378*, 703–706.
(3) Subramanian, S.; Zaworotko, M.J. *Angew. Chem., Int. Ed.* **1995**, *34*, 2127–2129.
(4) Yaghi, O.M.; Davis, C.E.; Li, G.; Li, H. *J. Am. Chem. Soc.* **1997**, *119*, 2861–2868.
(5) Li, H.; Davis, C.E.; Groy, T.L.; Kelley, D.G.; Yaghi, O.M. *J. Am. Chem. Soc.* **1998**, *120*, 2186–2187.
(6) Sauvage, J.P., Dietrich-Buchecker, C., Eds.; *Molecular Catenanes, Rotaxanes, and Knots*; Wiley-VCH: Weinheim, Germany, 1999.
(7) Gibson, H.; Bheda, M.C.; Engen, P.T. *Prog. Polym. Sci.* **1994**, *19*, 843–945.
(8) Amabilino, D.B.; Stoddart, J.F. *Chem. Rev.* **1995**, *95*, 2725–2828.
(9) Marand, E.; Hu, Q.; Gibson, H.W.; Veytsman, B. *Macromolecules* **1996**, *29*, 2555–2562.
(10) Fujita, M.; Kwon, Y.J.; Washizu, S.; Ogura, K. *J. Am. Chem. Soc.* **1994**, *116*, 1151–1152.
(11) Hoffart, D.J.; Loeb, S.J. *Angew. Chem., Int. Ed.* **2005**, *44*, 901–904.
(12) Davidson, G.J.E.; Loeb, S.J. *Angew. Chem., Int. Ed.* **2003**, *42*, 74–77.
(13) Oku, T.; Furusho, Y.; Takata, T. *Angew. Chem., Int. Ed.* **2004**, *43*, 966–969.
(14) Werts, M.P.L.; van den Boogaard, M.; Tsivgoulis, G.M.; Hadziioannou, G. *Macromolecules* **2003**, *36*, 7004–7013.
(15) Mason, P.E.; Bryant, W.S.; Gibson, H.W. *Macromolecules* **1999**, *32*, 1559–1569.
(16) Yamagishi, T.A.; Kawahara, A.; Kita, J.; Hoshima, M.; Umehara, A.; Ishida, S.I.; Nakamoto, Y. *Macromolecules* **2001**, *34*, 6565–6570.
(17) Kihara, N.; Hinoue, K.; Takata, T. *Macromolecules* **2005**, *38*, 223–226.
(18) van den Boogaard, M.; Bonnet, G.; van't Hof, P.; Wang, Y.; van Hutten, C.P.; Lapp, A.; Hadziioannou, G. *Chem. Mater.* **2004**, *16*, 4383–4385.

(19) Ooya, T.; Eguchi, M.; Yui, N. *J. Am. Chem. Soc.* **2003**, *125*, 13016–13017.
(20) Freeman, W.A.; Mock, W.L.; Shih, N.Y. *J. Am. Chem. Soc.* **1981**, *103*, 7367–7368.
(21) Day, A.I.; Blanch, R.J.; Arnold, A.P. WO 0068232 (2000) p 8.
(22) Kim, J.; Jung, I.S.; Kim, S.Y.; Lee, E.; Kang, J.K.; Sakamoto, S.; Yamaguchi, K.; Kim, K. *J. Am. Chem. Soc.* **2000**, *122*, 540–541.
(23) Day, A.I.; Blanch, R.J.; Arnold, A.P.; Lorenzo, S.; Lewis, G.R.; Dance, I. *Angew. Chem., Int. Ed.* **2002**, *41*, 275–277.
(24) Flinn, A.; Hough, G.C.; Stoddart, J.F.; Williams, D.J. *Angew. Chem. Int. Ed.* **1992**, *31*, 1475–1477.
(25) Zhao, J.Z.; Kim, H.J.; Oh, J.; Kim, S.Y.; Lee, J.W.; Sakamoto, S.; Yamaguchi, K.; Kim, K. *Angew. Chem., Int. Ed.* **2001**, *40*, 4233–4235.
(26) Sanjita, S.; Mantosh, K.; Sinha, E.K. *Org. Lett.* **2004**, *6*, 1225–1228.
(27) Lu, L.B.; Zhang, Y.Q.; Zhu, Q.J.; Xue, S.F.; Tao, Z. *Molecules* **2007**, *12*, 716–722.
(28) Jon, S.Y.; Selvapalam, N.; Oh, D.H.; Kang, J.K.; Kim, S.Y.; Jeon, Y.J.; Lee, J.W.; Kim, K. *J. Am. Chem. Soc.* **2003**, *125*, 10186–10187.
(29) Isobe, H.; Sato, S.; Nakamura, E. *Org. Lett.* **2002**, *4*, 1287–1289.
(30) Day, A.I.; Arnold, A.P.; Blanch, R.J. *Molecules* **2003**, *8*, 74–84.
(31) Zhao, Y.J.; Xue, S.F.; Zhu, Q.J.; Tao, Z.; Zhang, J.X.; Wei, Z.B.; Long, L.S.; Hu, M.L.; Xiao, H.P.; Day, A.I. *Chin. Sci. Bull.* **2004**, *49*, 1111–1116.
(32) Zheng, L.M.; Zhu, J.N.; Zhang, Y.Q.; Tao, Z.; Xue, S.F.; Zhu, Q.J.; Wei, Z.B.; Long, L.S. *Chin. J. Inorg. Chem.* **2005**, *21*, 1583–1588.
(33) Lagona, J.; Mukhopadhyay, P.; Chakrabarti, S.; Isaacs, L. *Angew. Chem., Int. Ed.* **2005**, *44*, 4844–4870.
(34) Park, K.M.; Whang, D.; Lee, E.; Heo, J.; Kim, K. *Chem. Eur. J.* **2002**, *8*, 498–508.
(35) Tuncel, D.; Steinke, J.H.G. *Macromolecules* **2004**, *37*, 288–302.
(36) Sindelar, V.; Moon, K.; Kaifer, A.E. *Org. Lett.* **2004**, *6*, 2665–2668.
(37) Whang, D.; Heo, J.; Kim, C.A.; Kim, K. *Chem. Commun.* **1997**, 2361–2362.
(38) Whang, D.; Kim, K. *J. Am. Chem. Soc.* **1997**, *119*, 451–452.
(39) Masson, E.; Lu, X.Y.; Ling, X.X.; Patchell, D.L. *Org. Lett.* **2009**, *11*, 3798–3801.
(40) Mukhopadhyay, P.; Zavalij, P.Y.; Isaacs, L. *J. Am. Chem. Soc.* **2006**, *128*, 14093–14102.
(41) Dai, L.P.; Tao, Z.; Zhu, Q.J.; Xue, S.F.; Zhang, J.X.; Zhou, X. *Acta Chim. Sinica* **2004**, *62*, 2431–2440.
(42) *Bruker*, *SAINT and SADABS*; Bruker AXS Inc.: Madison, WI, USA, 2005.
(43) Sheldrick, G.M. *Acta Cryst.* **2008**, *A64*, 112–122.
(44) Xu, Z.Q.; Yao, X.Q.; Xue, S.F.; Zhu, Q.J.; Tao, Z.; Zhang, J.X.; Wei, Z.B.; Lomg, L.S. *Acta Chim. Sinica.* **2004**, *62*, 1927–1934.
(45) Fu, H.Y.; Xue, S.F.; Zhu, Q.J.; Tao, Z.; Zhang, J.X.; Day, A.I. *J. Incl. Phenomenol. Macro.* **2005**, *52*, 101–107.
(46) Liu, S.M.; Ruspic, C.; Mukhopadhyay, P.; Chakrabarti, S.; Zavalij, P.Y.; Isaacs, L. *J. Am. Chem. Soc.* **2005**, *127*, 15959–15967.
(47) Mock, W.L.; Shih, N.Y. *J. Org. Chem.* **1983**, *48*, 3618–3619.
(48) Mock, W.L.; Shih, N.Y. *J. Org. Chem.* **1986**, *51*, 4440–4446.
(49) Meschke, C.; Buschmann, H.J.; Schollmeyer, E. *Thermochim. Acta* **1997**, *297*, 43–48.